Numerical Methods in Civil Engineering

Journal Homepage: https://nmce.kntu.ac.ir/

Investigating Concrete Arch Dam Behavior Under Underwater Explosion (Case Study: Karun4 Dam)

Reza Tarinejad [*], Hesane Ghanbari [**], Ramtin Sobhkhiz Foumani [***]

ARTICLE INFO

RESEARCH PAPER

Article history:
Received:
April 2022
Revised:
June 2023
Accepted:
December 2023

Keywords:
Air Blast,
Nonlinear Dynamic Analyses,
Dam-Reservoir-Foundation Interaction,
Karun-4 Dam

Abstract:

Studying the responses of dams to explosion-induced loads and evaluating their overall safety under such loads is highly significant regarding the strategic importance of dams. The present study investigates TNT-induced wave effects on the Karun-4 Dam in Iran. For this purpose, dynamic analyses were carried out on the dam reservoir and foundation system via the finite element method (FEM) in ABAQUS. The CONWEP theory allows the imposition of pressure loading caused by an explosion in the air. The reservoir was considered empty, and then three different heights of 225, 115, and 5 m were analyzed. The failure explosive weights of the three heights were calculated by trial and error. Analyses were performed with 1000, 1200, and 1300 kg of TNT for the height of 225 m, 1900, 1950, and 2000 kg of TNT for the height of 115, and 1800, 1900, and 2000 kg of TNT for the height of 5 m. It was observed that the dam failed at loads of 1300, 2000, and 2000 kg of TNT when the explosion occurred at 225, 115, and 5 m, respectively. The analyses were performed based on these loads. The results indicated that the reservoir water level had a negligible effect on the arch dam's failure blast load. Moreover, analysis results of the dam-reservoir-foundation system in filled-up and empty reservoir cases suggest that the failure explosive loads of filled-up and empty reservoir dams do not significantly differ, and the failure explosive load of the filled-up case is slightly lower than that of the empty case. For example, at an explosion height of 225 m, the failure load of the filled-up reservoir case was derived to be 1500 kg of TNT, while that of the empty reservoir case was obtained to be 1300 kg of TNT.

1. Introduction

Dams are among the most critical human-made structures. They are constructed at high expenses to supply water for drink, agriculture, and industries, control floods, and generate hydroelectric power. Given the importance of dam structures and their high costs, evaluating their safety under blast loads is crucial. A dam's response to a blast load depends on the blast-released energy, so destructive consequences will be imposed if it cannot resist these loads. The seismic response of concrete gravity dams has been a significant research topic for decades regarding dam safety concerns during earthquakes [1-2].

Ramajeyathilagam et al. in 2004 compared underwater blasts' experimental and numerical effects on a thin rectangular [3].

plate with specific dimensions. Sprague et al. in 2006 conducted a spectral-element finite element (FEM) analysis on a ship-like structure subjected to underwater blast loading [4]. Fallahzadeh et al. in 2008 studied the effects of an explosion on the surface and underground structures [5]. Langrand et al. in 2009 evaluated the body integration of a submarine subjected to underwater blast loading [6]. Mohtashami et al. in 2010 evaluated the behavior of steel frames under blast loading. They analyzed a three-story steel moment frame under blast loads [7]. Guzas et al. in 2010 simulated the response of a structure subjected to air blast [8]. Shoushtari et al. in 2011 performed a dynamic analysis on asymmetric structures under blast loads [9]. Mortezaei in

**** Professor of Civil Engineering Department, University of Tabriz, Tabriz, Iran*
*** PhD Student of Civil Engineering Department, University of Urmia, Urmia, Iran*
**** Corresponding Author: PhD Student of Civil Engineering Department, University of Qom, Qom, Iran* Sobhkhizarman@yahoo.co.uk

https://doi.org/10.61186/NMCE.461.3

2012 evaluated the performance of reinforced concrete columns subjected to an explosion [10]. Zhang et al. in 2013 numerically studied the rupture modes of a concrete gravity dam subjected to an underwater blast [11]. Wang et al. in 2014 investigated wave propagation and cavitation effects under the near-boundary blast [12]. Wang et al. in 2014 predicted damages imposed on a concrete gravity dam under explosion [13]. Norouzi et al. in 2015 numerically modeled the effects of in-reservoir blast loads on the dynamic behavior of concrete gravity dams [14].

Mostafaei et al. in 2020 argued that the material nonlinearity did not significantly affect the abutment's stability analysis. Therefore, the linear behavior is presumed for all materials (foundation rock, water, and concrete) [15].

A finite element modeling of arch dams subjected to underwater explosions. [16].

The behavior of the Karaj double curvature arch dam is studied, focusing on the effects of structural nonlinearity on the responses of the dam body when an underwater explosion occurs in the reservoir medium. Based on the results, the dam body responses are sensitive to inserting joints, and the constitutive model is considered for the dam body [17].

Furthermore, the dynamic response of concrete dams subjected to underwater contact explosion is studied using the LS-DYNA software in his study. The full coupled model was used based on the ALE (Arbitrary Lagrange-Euler) algorithm, including the propagation of shock waves and the interaction between water. The damage results show that it is worse when an explosive is in the water than when it is on the surface or at the bottom. With emphasis on the case that the explosive is in the water, the dynamic response of the concrete dam was simulated. The amount of energy absorbed by the dam, reservoir water, and dam foundation was obtained. The process of damage evolution of dam concrete and the major principal stress of the dam were presented. The analytical results show that the dam is prone to the most risks when the explosive is in the water and at a certain distance from the bottom [18].

Studies conducted on the effects of air blasts on dams primarily focus on commercial or residential buildings and structures. Also, studies regarding the blast effects on dams mainly focus on in-reservoir blasts. Thus, it is necessary to investigate the effects of blasts on dams as it is a new and essential practice. The finite element model of the Karun 4 dam-reservoir-support system has been created, and regarding the assumptions of this modeling, it can be mentioned that the support is a part of the sphere with a radius three times the dam's height. It is also assumed that the dam reservoir is modeled as a prism with a length equal to 3 times the dam's height.

On the other hand, because the normal level of the reservoir is higher than the pressure block on the right side of the dam, valve modeling has been done to maintain the normal level. The valve is modeled rigidly to avoid the effect of the valve on the modal and dynamic responses of the dam. Also, the support is considered as a mass, and the dam reservoir is modeled as an acoustic fluid. At the end of the tank, the infinite boundary condition is applied to prevent the return of the emitted waves. The acoustic pressure at the tank's surface is assumed to be zero throughout the analysis and as a boundary condition. Conwep theory has been used in explosion modeling. The interaction of the support tank dam has been included in the behavior modeling of the studied system under the effect of explosive load.

The purpose of this research is to consider the conditions of the dam structure in order to obtain realistic answers due to the explosion and modeling of the dam, reservoir, and support and considering their measurement effects.

2. Explosion

An explosion is the abrupt release of energy caused by gas combustion, nuclear explosion, or different types of bombs. The TNT unit is typically used as a reference to determine the power of an explosion. The essential characteristics of an explosion that apply loads on structures include accidental explosion location, dynamic and transient loads, and low effect time, which varies from a few milliseconds to a few seconds. Figure 1 illustrates explosion-induced pressure variations consisting of positive and negative phases.

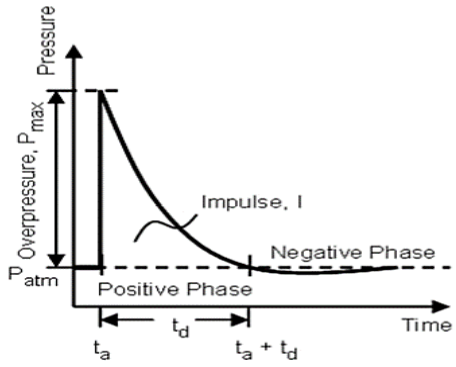

Fig. 1: The time history of air explosion-induced pressure

Brode in 1959 proposed an equation to calculate the pressure as [19].

$$P(t) = \begin{cases} 0 & t < t_a \\ P_{max}\left(1 - \frac{t - t_a}{t_d}\right)e^{-b\left(\frac{t-t_a}{t_d}\right)} & t_a \le t \le t_a + t_d \\ 0 & t > t_a + t_d \end{cases} \quad (1)$$

P(t) is the maximum pressure at time t after the explosion, Pmax is the pressure peak, ta is the time the shock wave is imposed, *td* is the time required by the shock wave to reach Pmax, and b is the decay constant. Pmax is the maximum difference between the explosion-side pressure Ps and reflected pressure Pr (Brode,1959) [21].

2.1. Air explosion scale types

Two scales have been employed for air explosion: Sach and Hopkinson. The Sach scale has a more general use than the Hopkinson scale. The Sach scale is mainly used to predict the characteristics of large explosion waves, such as nuclear explosions. The present study adopted the Hopkinson scale since it investigates typical explosives. According to the Hopkinson scale, when two explosives of the same material explode in the same condition, their shock wave effects are represented as term Z.

$$Z = \frac{R}{W^{\frac{1}{3}}} \tag{2}$$

R is the distance from the explosion center, and W is the explosive's weight. Equation (1) applies to 1 kg of an explosive or 1 pound of TNT [8].

2.2 Air explosion parameters

The air explosion parameter equations were adapted from the modified equations proposed by Guzas and Earls in 2010 [8]. The explosive loading time is calculated as:

$$\frac{t_d}{W^{\frac{1}{3}}} = \frac{980\left[1+\left(\frac{Z}{0.54}\right)^{10}\right]}{\left[1+\left(\frac{Z}{0.02}\right)^{3}\right]\left[1+\left(\frac{Z}{0.74}\right)^{6}\right]\sqrt{1+\left(\frac{Z}{6.9}\right)^{2}}} \tag{3}$$

where *td* is the time of the explosion profile's positive phase in seconds. Ps, which is the pressure peak that is directly applied to the structure, is calculated as:

$$P_s = 808P_{atm}\frac{\left[1+\left(\frac{Z}{4.5}\right)^{2}\right]}{\sqrt{\left[1+\left(\frac{Z}{0.048}\right)^{2}\right]\left[1+\left(\frac{Z}{0.32}\right)^{2}\right][1+]}} \tag{4}$$

where P_s is the extra pressure applied to the structure in bars, P_{atm} is the atmospheric pressure in bars, and z is the scaled distance.

It is much easier to calculate P_s than P_r. Wang and Zhang in 2014 proposed that. [22].

$$P_r = P_s\left(2+\frac{6P_s}{P_s+7P_{atm}}\right) \qquad P_s < 6.9 \text{ bar} \tag{5}$$

where P_r is the maximum reflected extra pressure, P_s is the extra pressure, and P_{atm} is the atmospheric pressure.

Air molecules begin to interact when $P_s \geq 6.9$ bar and the air can no longer be assumed to be an ideal gas. In this case, Wang and Zhang in 2014 proposed the equation below: [12]

$$P_r = P_s\left[\frac{0.03851\,P_s}{1+0.0025061\,P_s+4.041\times10^{-7}\,P_s^{\,2}}+2+\frac{0.004218+0.7011\,P_s+0.001442\,P_s^{\,2}}{1+0.1160\,P_s+8.086\,10^{-4}\,P_s^{\,2}}\right] \tag{6}$$

where P_s is the maximum extra pressure in bars [8].

3.Validation

The model proposed by Guzas and Earls in 2010 was modeled in ABAQUS to validate the present study's explosion model [8]. The model was a steel plate with dimensions of 3.18 mm × 9.14 mm × 9.14 mm. Figure 2 shows the meshed model. An explosion load of 1.36 kg of TNT was applied to the plate at a distance of 1.52 m. Table 1 provides the Johnson-Cook parameters of the steel plate.

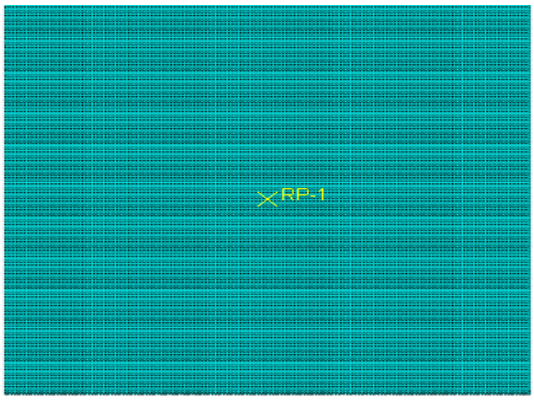

Fig. 2: The FEM of the steel plate

Table 1: Material properties of steel plate

Plastic properties					Elastic properties		
A	B	C	N	$\dot{\varepsilon_0}$	E	r	**ν**
MPa	MPa			$1/s$	GPa	kg/m^3	
319	554	0.0327	0.135	0.0057	209	7850	**0.3**

Figure 3 represents the air blast-induced pressure's time history curve. Also, Figure 4 compares the displacement-time history curves of the plate center. As can be seen, the model is in good agreement with [8] suggesting that the blast load was correctly modeled. The difference observed in the displacement of the plane's center is due to the difference in the assumptions used in the analysis and the discrete numerical method.

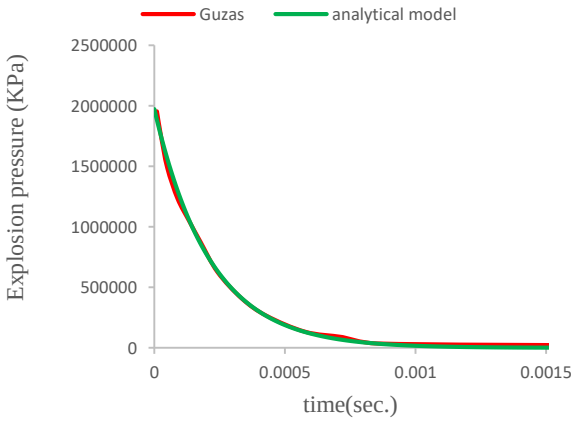

Fig. 3: Comparison of the time history of the air blast pressure

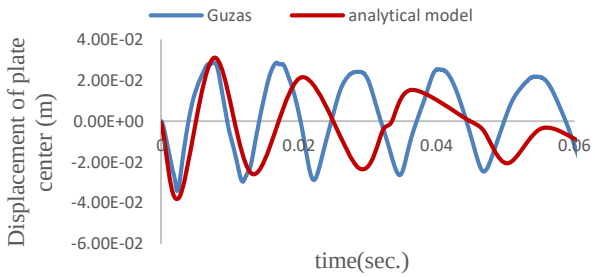

Fig. 4: Comparison of the displacement for the center of the plate

4. Explosion effects on Karun-4 dam

The double-curvature arch dam of Karun-4 is located in Chaharmahal and Bakhtiari Province, 180 km west-south of Shahrekord and 4 km downstream of the intersection of Armand and Bazoft Rivers. Karun-4 Dam has a height and a crest length of 230 and 440 m, respectively. Moreover, the thickness of the Karun-4 Dam is 7 and 52 m at the crest and foundation counters, respectively. Figure 5 demonstrates the Karun-4 Dam.

Fig. 5: A view of the arched concrete dam of Karun 4

4.1. Element sensitivity analysis

Since the element size largely influences the accuracy of explosion responses, several meshing stages were applied to obtain a proper element size and minimize the difference between the maximum numerical explosion pressure and the maximum analytical pressure proposed in Equation (5) and Equation (6). The explosion pressure was calculated for the element sizes of 5.382699, 2.694036, and 0.673915 m. Then, the results were compared to analytical ones and found that an element size of 0.673915 posed an error of 9%. Thus, it was selected as a suitable size for the analysis. Figure 6 plots the explosion-induced pressure error versus the element size for a load of 1000 kg and a distance of 10 m.

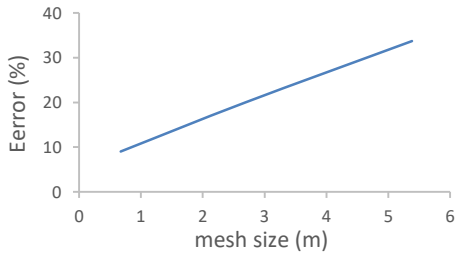

Fig. 6: Error estimation of air blast pressure error versus element size

4.2. The numerical model of Karun-4 Dam

The Karun double curvature dam with a height of 230 m has been modeled using 8156706 cubic elements. The compressive block at the right flank of the dam has been modeled using 300 cubic blocks. The dam reservoir has been considered acoustic, and its length has been assumed to be three times the dam's height. The reservoir of the Karun-4 dam has been modeled via 258977 tetrahedral elements. The infinite boundary condition has been applied at the reservoir's end to prevent the propagated waves' return. Notably, the dam-reservoir interaction has been considered by connecting their interface nodes. In addition, the dam foundation interaction has been taken into account. For this purpose, the foundation has been modeled as a hemisphere with a radius 3 times the dam's height. In this model, the dam foundation interaction has been considered mutual, similar to the dam-reservoir interaction. To model the foundation, 41131 4-node tetrahedral elements have been used. The infinite boundary condition has been considered at the outer surface of the foundation to prevent the return of waves into the model.

Given that the meshing of the whole dam body using elements with a size of 0.7 m prolongs the analysis time, the mesh with the 0.7-m size has been used for the regions in front of the explosives, and a mesh with a larger size has been used for other regions of the dam body. As such, 3 different mesh sizes have been used for 3 different positions of the explosives (5 m from the dam foundation, 115 m from the dam foundation, and 225 m from the dam foundation). When the explosives are located 5 m from the dam foundation, the bottom portion of the dam has been meshed with an element size of 0.7 m, and the other regions have a coarser mesh. For the case where the explosives are placed at 115 m from the dam foundation, the dimensions of the middle elements of the dam have been considered to be 0.7 m, and the rest of the parts have larger elements. Finally, for the case where the explosives are located 225 m from the dam foundation, the meshing of the top part near the dam crest has an element size of 0.7 m, and the rest of the regions have a coarser mesh. In the text, only the image of the mesh for the case with the explosive at 115 m from the dam foundation has been shown (Figures 7 and 8)

Figures 7 and 8 represent the FEM model of the Karun-4 dam reservoir-foundation system. Body contraction joins were ignored to avoid a long analysis time.

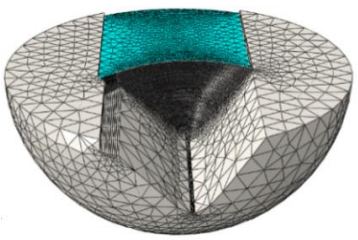

Fig. 7: The FEM of dam-reservoir-foundation for 115m height

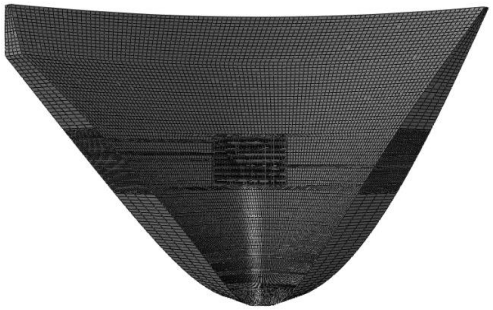

Fig. 8: The FEM of Karun4 dam, for 115m height

The element size should be very small in meshing. This consideration, however, increases the analysis time. Therefore, only the elements around the explosion location were made very small. As shown in Figure 8, 156,706 linear cubic elements were applied to the dam system. The foundation was considered part of a sphere with a radius of three times larger than the dam height. A total of 41131 four-node pyramid elements were applied to the foundation. The reservoir length was three times larger than the dam height, modeled using 258,977 linear four-node acoustic pyramid elements. In addition, the compressive block was modeled by 300 eight-node linear cubic elements. Table 2 illustrates the material specifications of the FEM model.

Table 2: Material properties of Karun4 dam

24 GPa	**Static elasticity modulus**	**Concrete**
30 GPa	Dynamic elasticity modulus	
0.2	Poisson ratio	
$2400\frac{kg}{cm^2}$	Density	
10 GPa	Dynamic elasticity modulus	**Rock**
0.3	Poisson ratio	
$2600\frac{kg}{cm^2}$	Density	
$1000\frac{kg}{cm^2}$	Density	**Water**
2.13 GPa	Bulk modulus	

The failure of the two main mechanisms, i.e., the tension-based failure mechanism and the compressive smashing-based failure mechanism, refers to failure in the concrete. Since the bodies of concrete dams are designed based on the non-tension principle, tiny tension cracks and damages occur in the dam bodies. Thus, uniaxial compression and tension concrete stress-strain curves are introduced to the software. Uniaxial stress-strain curves can be translated into plastic stress-strain curves that are automatically introduced to the software by users via given stress values and inelastic strain values. The plastic concrete damage model is employed as it can simulate the actual concrete behavior under tension and compression.

5. Results

The dam-reservoir-foundation system was analyzed under explosion loads at different heights, and the results were compared.

5.1. Explosion load cases

Explosion loads were investigated at different heights, including 225 m (near the crest), 115 m (in the middle of the dam), and 5 m (near the base). Several analyses were performed for each height to obtain the lowest dam failure load, based on which the outputs were calculated. The explosion location was considered to be 10 m from the dam for the entire study cases. The cases were investigated for both filled-up and empty reservoirs.

5.1.1. Dynamic analysis results for the filled-up reservoir

When the reservoir water level was normal, the dam system's response was analyzed at three explosion load heights, including 225, 115, and 15 m. The rupture-causing explosive weight was calculated by trial and error. To this end, various analyses were carried out for different explosive weights, including 1000, 1500, and 2000 kg of TNT at the height of 225 m, 1900, 2000, and 3000 kg of TNT at the height of 115 m and 1500, 1900, and 2000 kg of TNT at the height of 5 m. The filled-up dam failed under the explosion loads of 1500, 2000, and 1800 kg of TNT at 225, 115, and 5 m heights, respectively.

5.1.1.1. Displacement

Figures 9, 10, and 11 illustrate the displacement curves of the crest and the explosive mass level at three different heights. As shown in Figure 10, the difference between the displacement curves is minimal since the explosion location is near the crest. Moreover, the displacement peaks occurred at almost the same time. According to Figure 11, since the explosive height of 115 m is distant from the crest, the maximum displacement moments of the crest and the explosion location differ. The maximum crest displacement occurred at 0.4 s. According to Figure 12, due to the considerable distance between the crest and the explosion location, the explosion location's displacement peak took place in a short time, while that of the crest occurred at 0.73 s, which is two times larger than that of the case with the explosion location in the middle of the dam. A comparison of the displacement values at the three heights indicates that the maximum displacements were approximately 3.12 mm toward the dam, 1.8 mm toward the downstream, and 0.6 mm at the heights of 225, 115, and 5 m, respectively. The maximum displacement of the explosive mass level was the

highest at the height of 225 m, followed by those at 115 and 5 m, respectively.

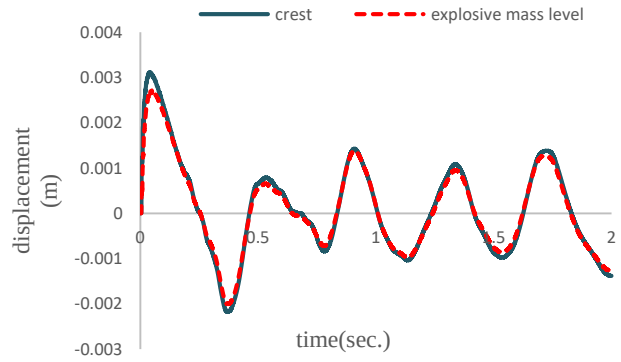

Fig. 9: Displacement time history in 225m height

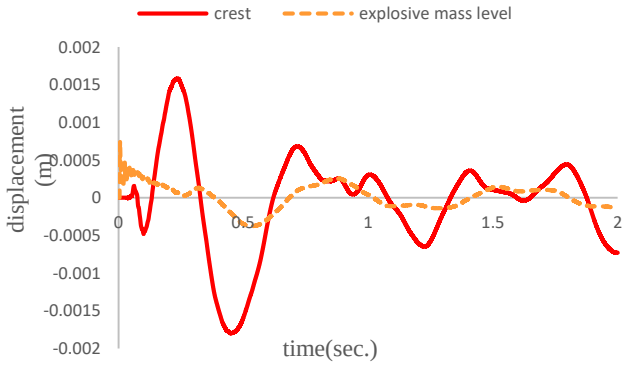

Fig. 10: Displacement time history in 115m height

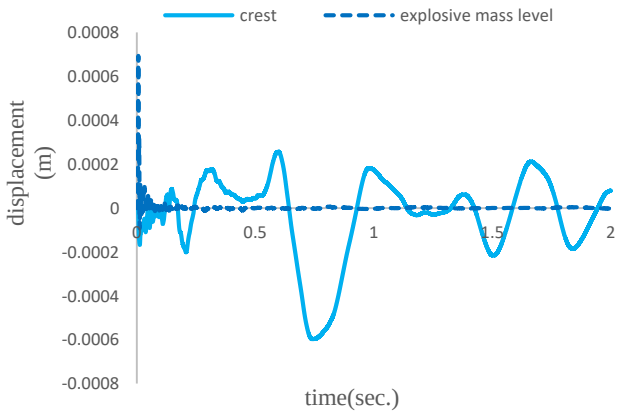

Fig. 11: Displacement time history in 5m height

5.1.1.2. Stress

Figures 12, 13, and 14 demonstrate stress contours for the three heights and the two cases at the maximum displacement moment and at t=1s. When the maximum displacement occurred, the stress was obtained to be 0.732, 0.1810, and 0.03842 MPa at the explosion heights of 225, 115, and 5 m, respectively. Figures 16-18 illustrate the crest and base stress contours for each height value. As can be seen, the maximum crest stress was obtained to be 2.13 MPa at the explosion height of 225 m because the explosion load was close to the crest.

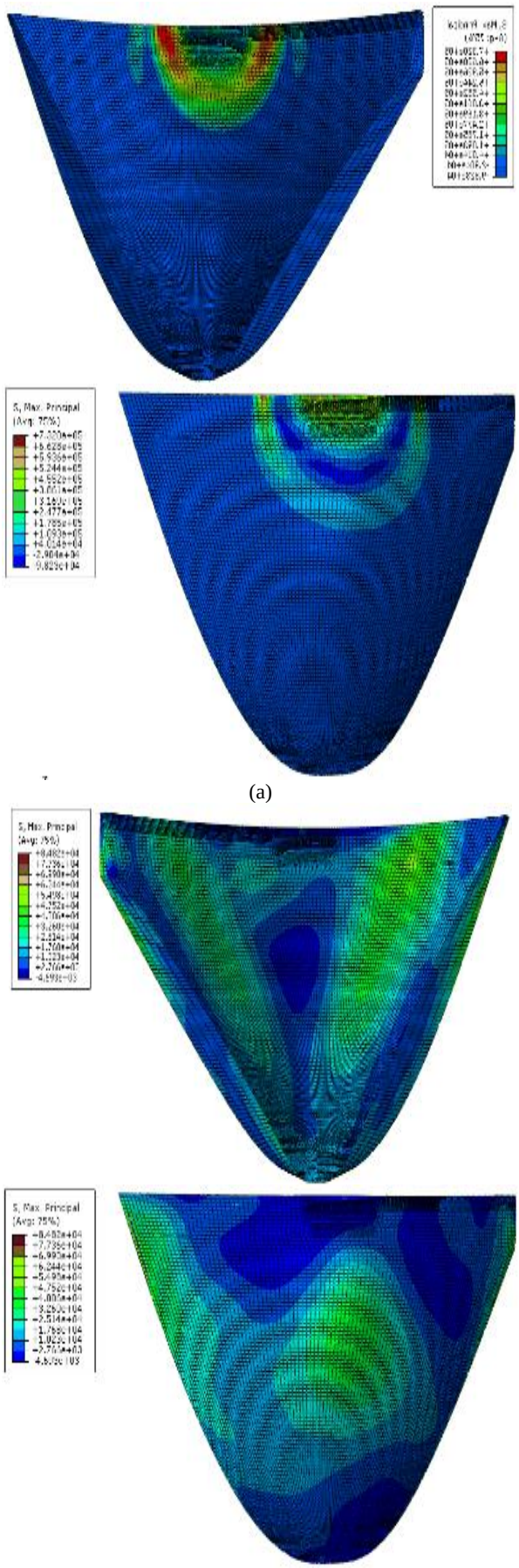

(a)

(b)

Fig. 12: Stress distribution contours for an explosion height of 225 m: a) at the maximum displacement moment, and b) at t = 1s

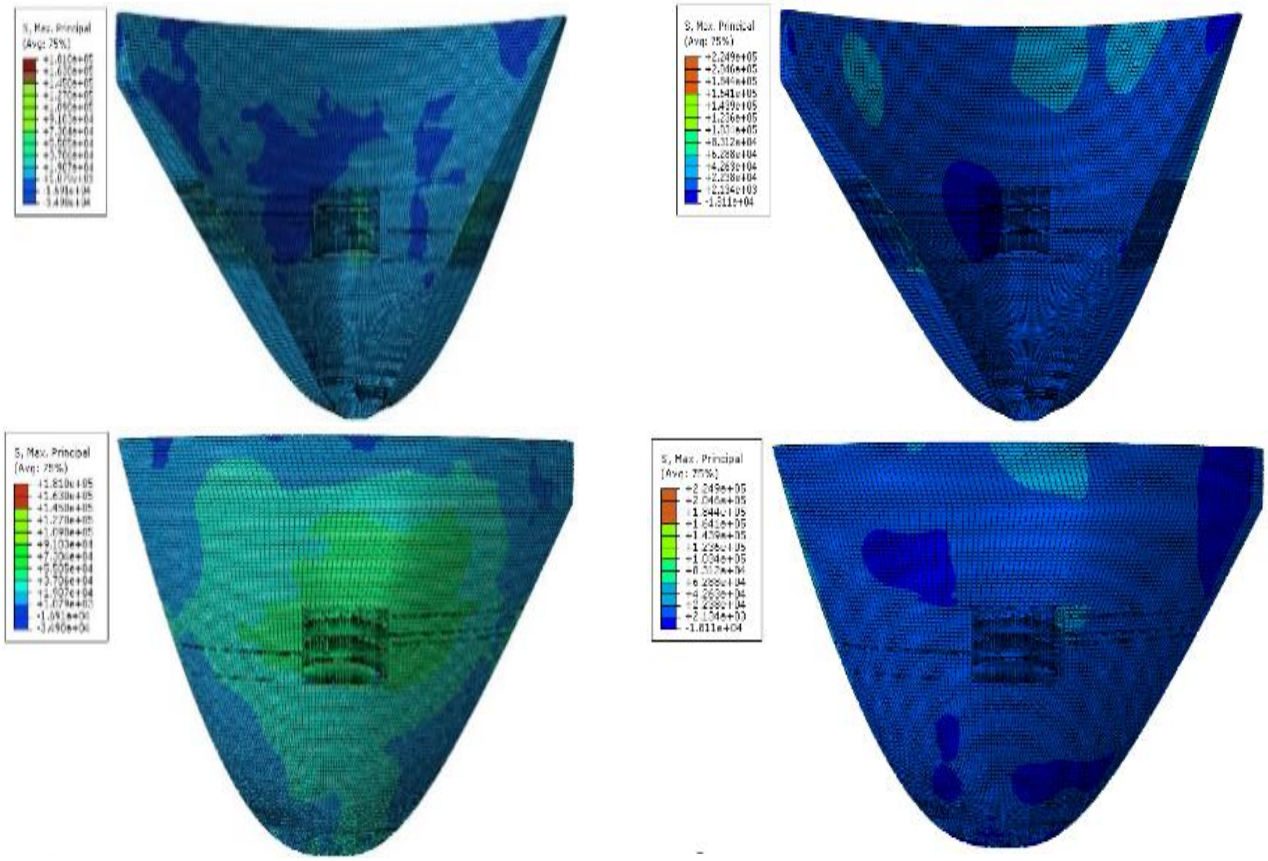

(a) (b)

Fig. 13: Stress distribution contours for an explosion of 115 m: a) at the maximum displacement moment and b) at t = 1s

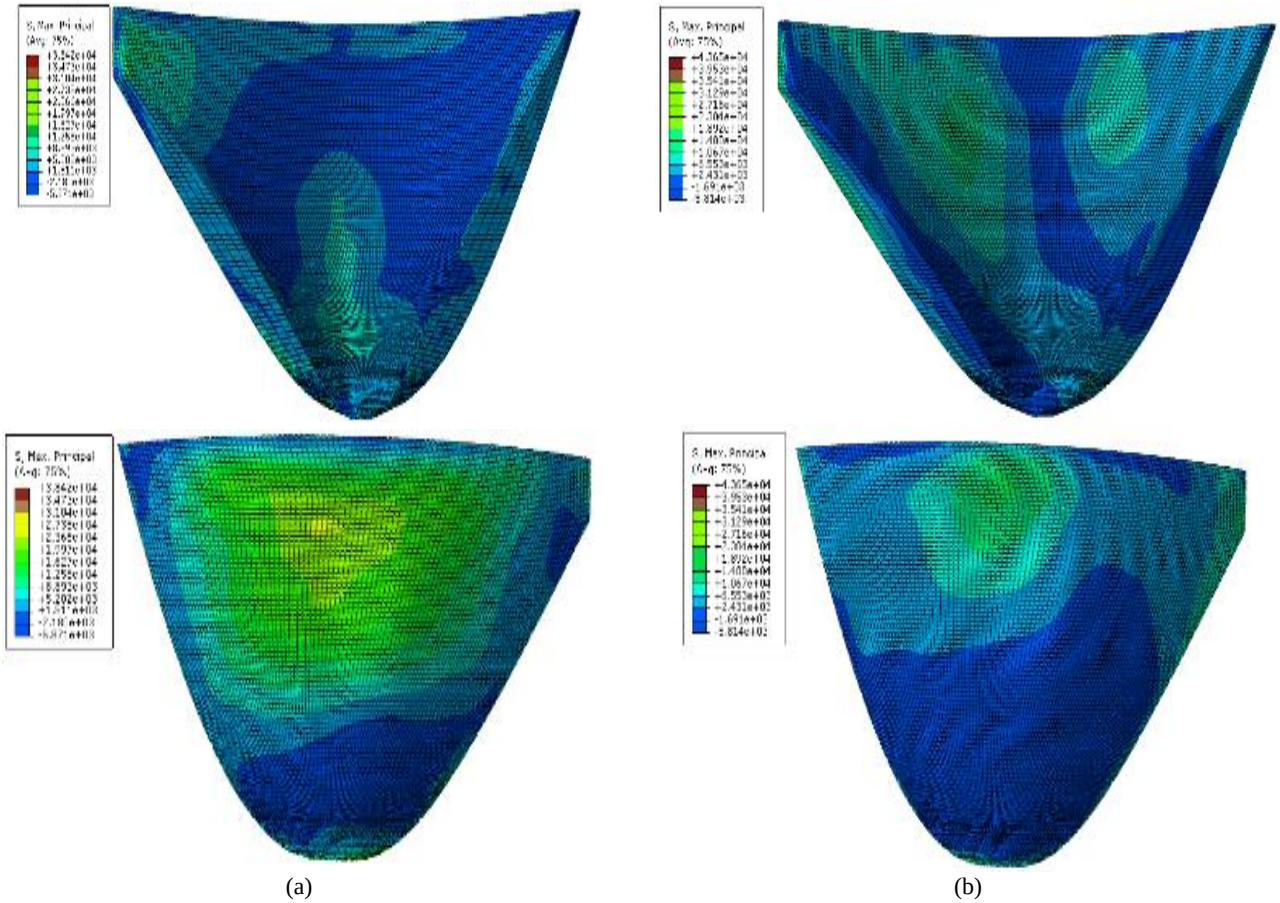

(a) (b)

Fig. 14: Stress distribution contours for an explosion of 5 m: a) at the maximum displacement moment and b) at t = 1s

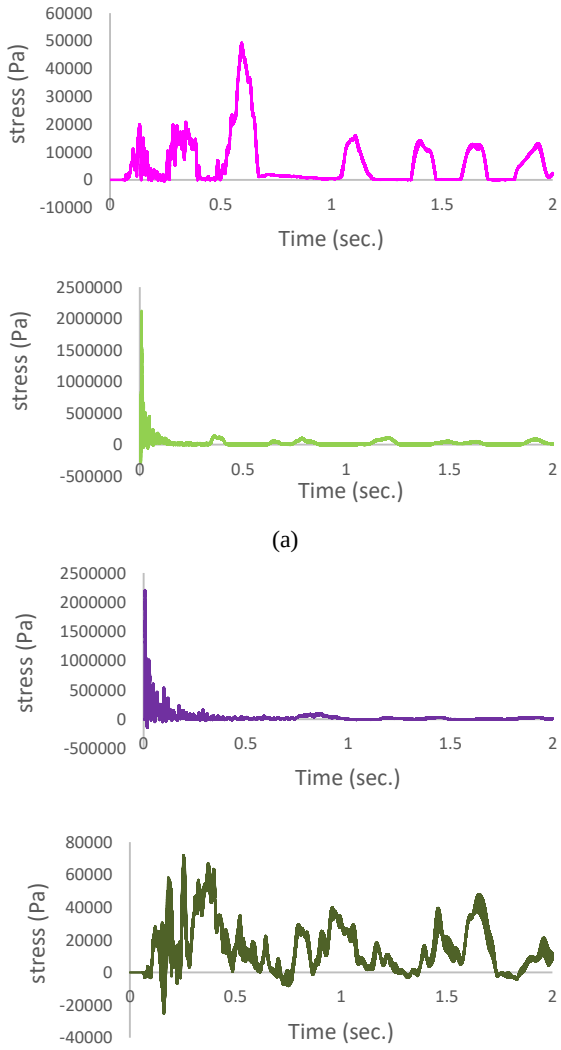

Fig. 15: Stress time history at an explosion of 225 m in a) crest and b) base

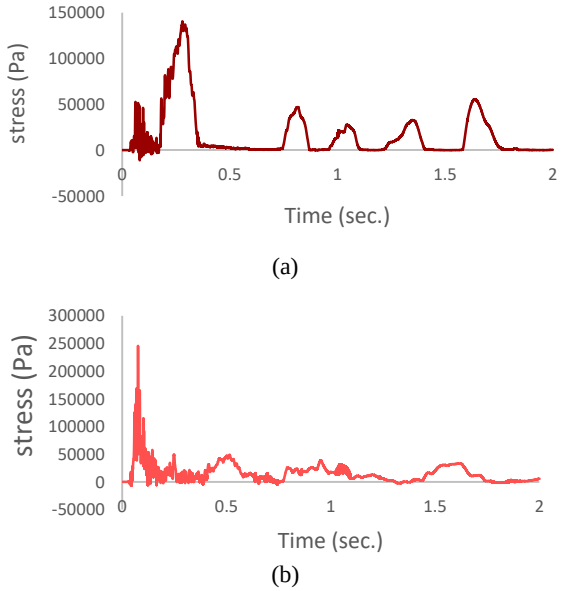

Fig. 16. Stress time history at an explosion of 115 m in a) crest and b) base

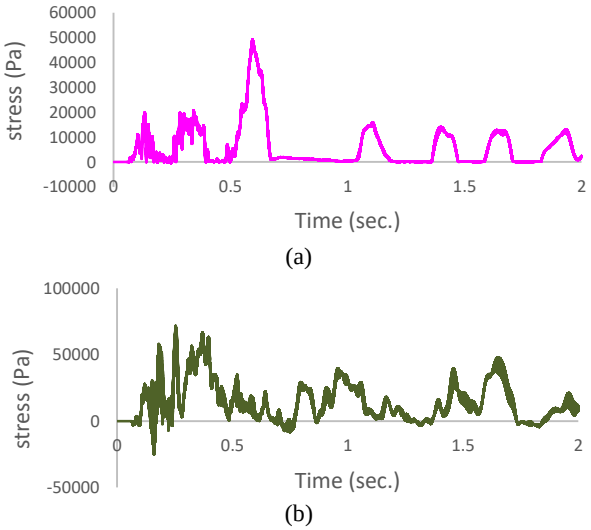

Fig. 17: Stress time history at an explosion of 5 m in a) crest and b) base

5.1.2. Dynamic analysis results for the empty reservoir

The reservoir was considered empty, and then three different heights of 225, 115, and 5 m were analyzed. The rupture explosive weights of the three heights were calculated by trial and error. Analyses were performed with 1000, 1200, and 1300 kg of TNT for the height of 225 m, 1900, 1950, and 2000 kg of TNT for the height of 115, and 1800, 1900, and 2000 kg of TNT for the height of 5 m. It was observed that the dam failed at loads of 1300, 2000, and 2000 kg of TNT when the explosion occurred at 225, 115, and 5 m, respectively. The analyses were performed based on these loads.

5.1.2.1. Displacement

Figures 18, 19, and 20 represent the time histories of the crest and explosive mass level displacements at the three heights. As shown in Figure 19, the crest and explosive mass level displacements are close since the explosion location was near the crest. Moreover, the maximum displacement moments of both cases happened in a very short time. According to Figures 19 and 20, due to the distance between the crest and the explosion location, the maximum explosive mass level displacement occurred within a short time after the maximum crest displacement. A comparison of the maximum crest displacements at the three heights reveals that the highest displacement occurred at 225 m since the explosion location was close to the crest. The explosive mass level displacement was calculated to be 2.55, 0.75, and 0.74 mm at 225, 115, and 5 m, respectively.

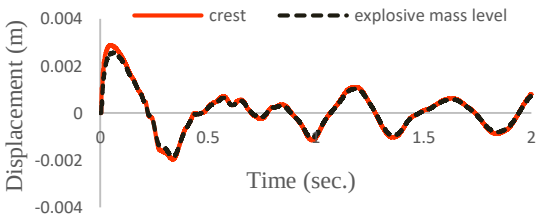

Fig. 18: The displacement time histories at an explosion height of 225 m

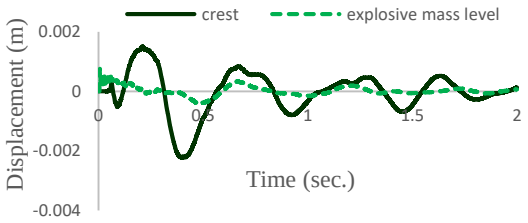

Fig. 19: The displacement time histories at an explosion height of 115 m

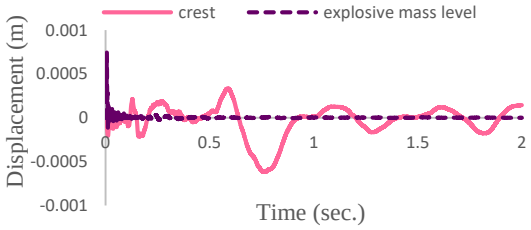

Fig. 20: The displacement time histories at an explosion height of 5 m

5.1.2.2. Stress

Figures 21, 22, and 23 depict stress contours at 225, 115, and 5 m explosion heights, respectively. As can be seen, when the highest displacement occurred, the highest stress was derived to be 0.5683 MPa at the height of 225 m, followed by the stress values of 0.1558 and 0.05386 MPa at the heights of 115 and 5 m, respectively.

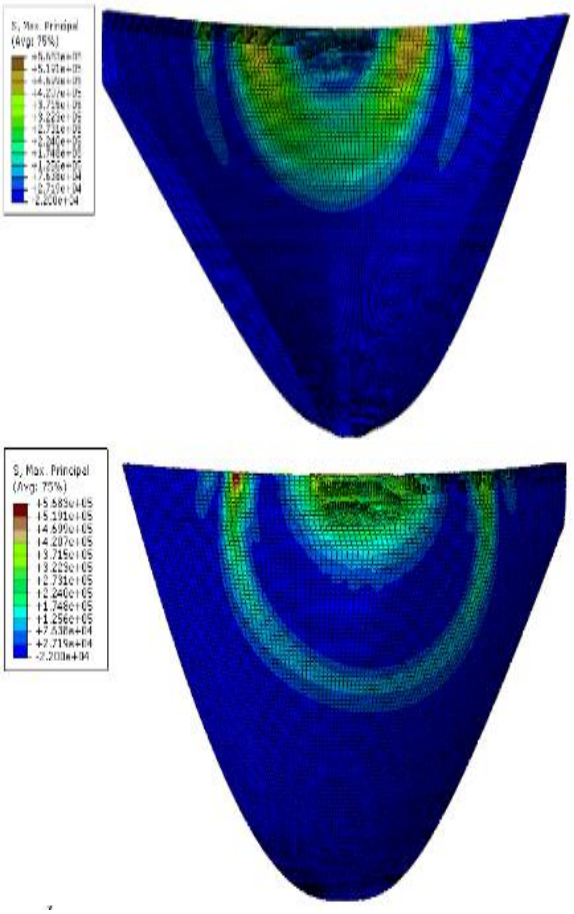

(a)

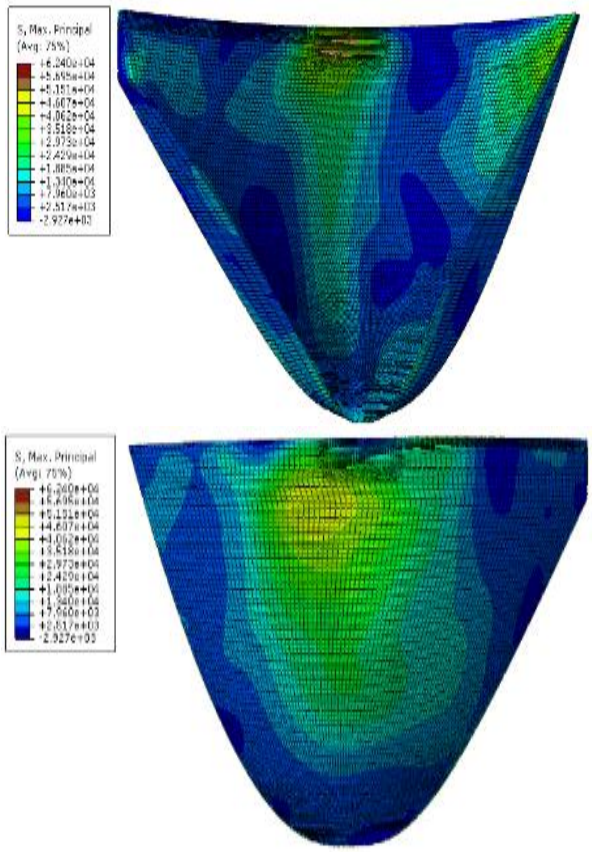

(b)

Fig. 21: Stress distribution contours for an explosion height of 225m at a) maximum displacement moment and b) t=1 s

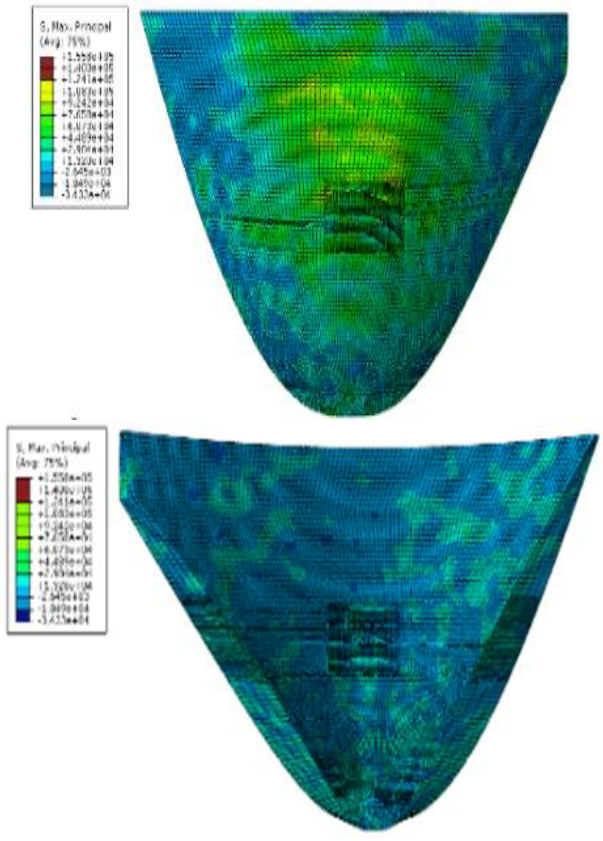

(a)

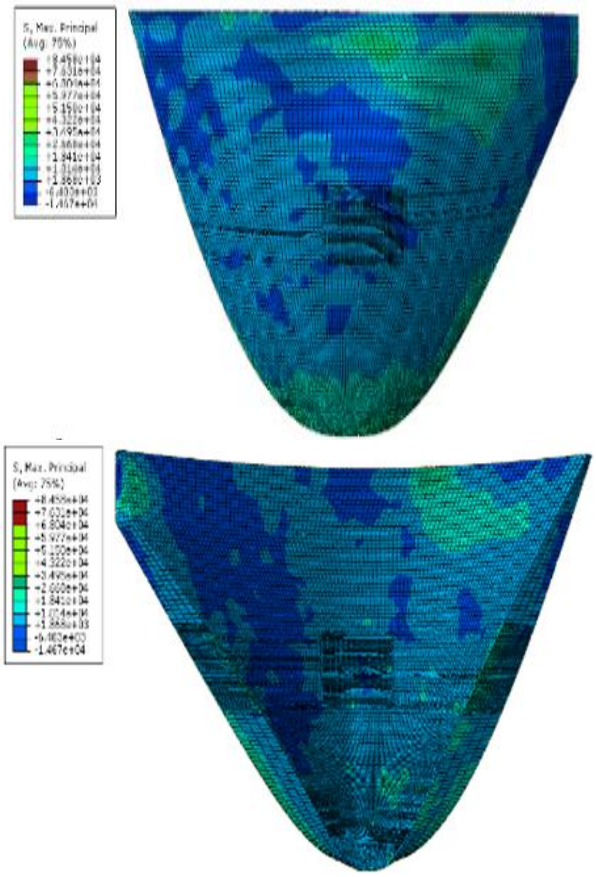

(b)

Fig. 22: Stress distribution contours for an explosion height of 115m at a) maximum displacement moment and b) t=1 s

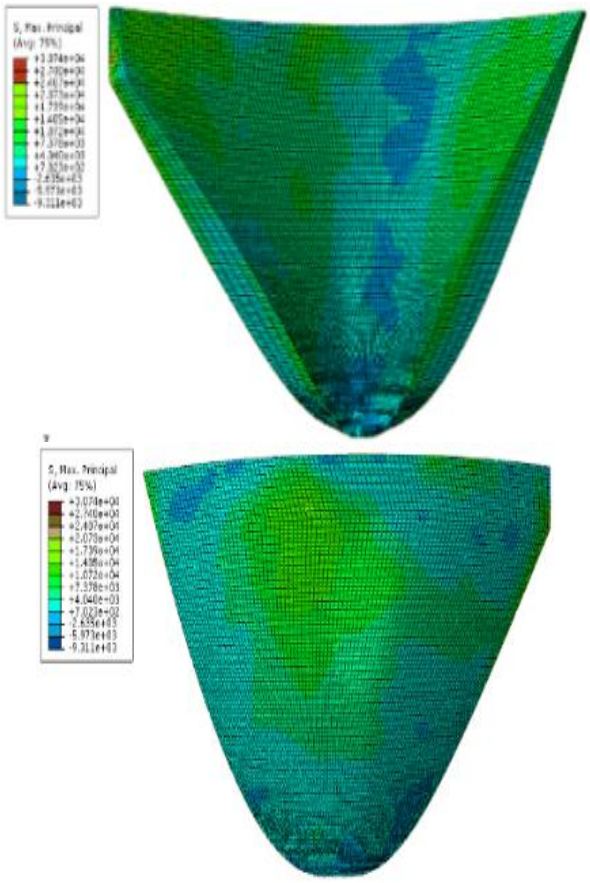

(b)

Fig. 23: Stress distribution contours for an explosion height of 5m at a) maximum displacement moment and b) t=1 s

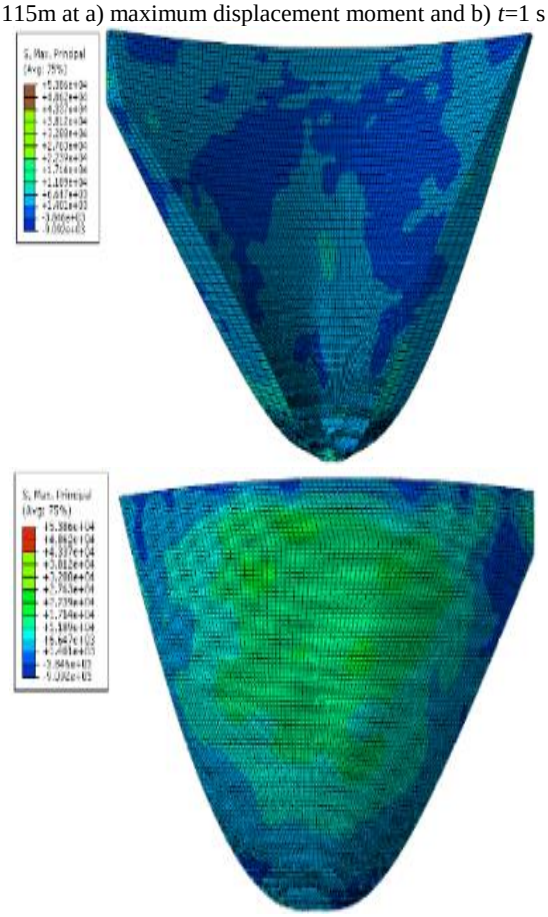

(a)

Figures 24-26 illustrate the stress diagrams. As can be seen, the dam base's maximum stress happened at an explosion height of 5 m.

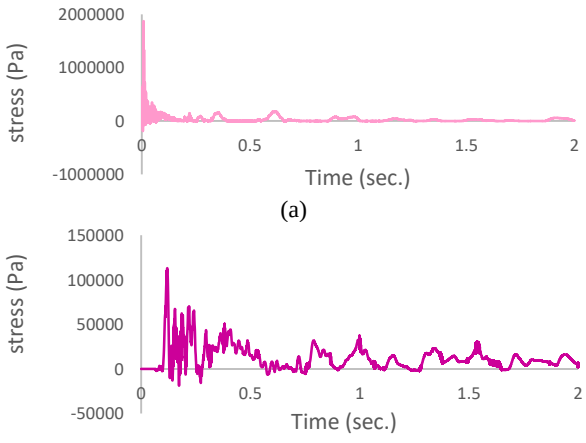

(a)

(b)

Fig. 24: Stress distribution in 225 m height. a) dam crest. b) dam base

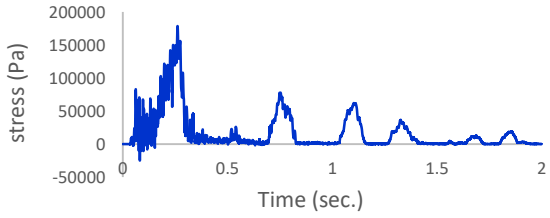

(a)

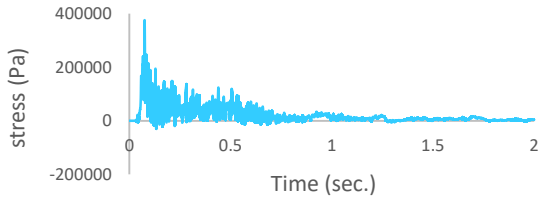

(b)

Fig. 25: Stress distribution in 115 m height. a) dam crest. b) dam base

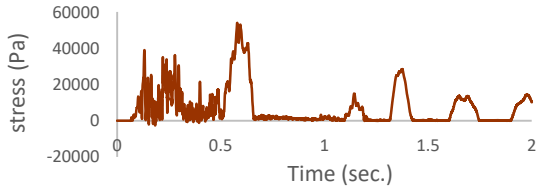

(a)

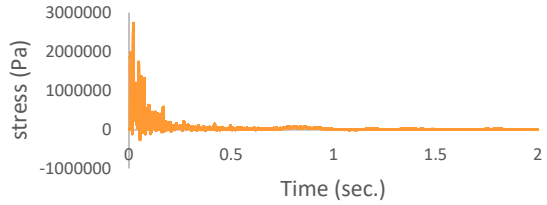

(b)

Fig. 26: Stress distribution in 5 m height. a) dam crest. b) dam base

6. Conclusion

The present study proposed a three-dimensional model for the dam-reservoir-foundation system of Karun-4 Dam under peripheral explosion. Simulations were performed at three heights and in the two cases of filled-up and empty reservoirs while considering nonlinear behavior for the dam material. The results largely depended on element size in analyzing the dam-reservoir-foundation system subjected to an explosion. To validate the element size, element sensitivity analyses were carried out, and it was found that an element size of 0.67 m is suitable with an error of below 10%. Smaller elements were applied to those parts of the dam subjected to the explosion, while larger elements were used for other parts to cut the computation time short. The dam ruptured at loads of 1500, 2000, and 1800 kg of TNT when the explosion happened at a height of 225, 115, and 5 m, respectively. The explosive load of the dam middle's rupture was 2000 kg of TNT for both filled-up and empty reservoirs. In addition, the explosive failure loads of the dam's crest were 1500 and 1300 kg of TNT for filled-up and empty reservoirs, respectively. An explanation for the higher failure load in the middle section of the dam than its base is the higher stiffness of the middle part than that of the crest. According to the analysis results, the crest displacement for an explosion height of 225 m was 3.12 and 2.7 mm in the filled-up and empty reservoirs, respectively. Also, the crest displacement was higher at an explosion height of 225 m than at heights of 115 and 5 m.

The analysis results of the dam-reservoir-foundation system in filled-up and empty reservoir cases suggest that the failure explosive loads of filled-up and empty reservoir dams do not significantly differ, and the failure explosive load of the filled-up case is slightly lower than that of the empty case. For example, at an explosion height of 225 m, the failure load of the filled-up reservoir case was derived to be 1500 kg of TNT, while that of the empty reservoir case was obtained to be 1300 kg of TNT.

5. References

[1] Mostafaei H, Behnamfar F, Alembagheri M. (2022). Reliability and sensitivity analysis of wedge stability in the abutments of an arch dam using artificial neural network. Earthquake Engineering and Engineering Vibration. 21(4):1019-33.

[2] Mostafaei H, Behnamfar F. (2021). Wedge Movement Effects on the Nonlinear Behavior of an Arch Dam Subjected to Seismic Loading. International Journal of Geomechanics. 1;22(3):04021289.

[3] Ramajeyathilagam K. & Vendhan C.P. (2004). Deformation and rupture of thin rectangular plates subjected to underwater shock, International Jornal Impact Engineering, 30, 699-719.

[4] Sprague M.A. & Geers T.L. (2006). A spectral-element/finite-element analysis of a ship-like structure subjected to an underwater explosion, Computer methods in applied mechanics and engineering,19, 2149-2167.

[5] Fallahzadeh P. & Baziar M. (2008). Investigation explosion effect on underground structures,14th national conference on civil engineering students, Semnan university, Iran. (In Persian)

[6] Langrand B., Leconte N., Menegazzi A. & Millot T. (2009). Submarine hull integrity under blast loading, International Journal of Impact Engineering, 36,1070-1077.

[7] Mohtashami E. Sinayi S. & Shushtari A. (2010). Evaluating steel frames behavior under blast loading; 5th national congress on civil engineering, Ferdowsi University of Mashhad, Mashhad, Iran.

[8] Guzas E.L. & Earls C. J. (2010). Air blast load generation for simulating structural response, Steel Composit Struct, 10, 429-455.

[9] Shushtari, A. & Salehabad M., (2011). Dynamic analysis of axisymmetric concrete buildings under blast loading, 6th national congress on civil engineering, Semnan University, Semnan, Iran (in Persian).

[10] Mortezayi, A. (2012). Evaluating retrofitted reinforced concrete column performance evaluation under explosion, 2nd national conference on Crisis Management, Tehran, Iran. (in Persian)

[11] Zhang S. Wang G. Wang C. Pang B. & Du C. (2013). Numerical simulation of failure modes of concrete gravity dams subjected to underwater explosion, Engineering Failure Analysis, 36, 49-64.

[12] Wang G. Zhang S. Yu M. Li H. & Kong Y. (2014). Investigation of the shock wave propagation characteristics and cavitation effects of underwater explosion near boundaries, Applied Ocean Research, 46, 40-53

[13] Wang G. & Zhang S. (2014). Damage prediction of concrete gravity dams subjected to underwater explosion shock loading, Engineering Failure Analysis, 39, 72-91.

[14] Noroozi F. Kalateh F. & Ghanbari H (2015). Numerical modeling of dynamic behavior of concrete gravity dams subjected to under water explosion, 10th international congress on civil engineering, University of Tabriz, Tabriz, Iran.

[15] Mostafaei H, Behnamfar F, Alembagheri M. (2020). Nonlinear analysis of stability of rock wedges in the abutments of an arch dam due to seismic loading. Structural monitoring and maintenance. 7(4):295-317.

[16] Zhu, F., Zhu, W.H., Zhu, X., Sun, J.B. and Hua, X. (2012), "Numerical simulation of arch dam withstand underwater explosion

[17] Moradi, M., Aghajanzadeh, S. M., Mirzabozorg, H., & Alimohammadi, M. (2018). Underwater explosion and its effects on nonlinear behavior of an arch dam. Coupled systems mechanics, 7(3), 333-351.

[18] Yu, T. (2009), "Dynamical response simulation of concrete dam subjected to underwater contact explosion load," Proceedings of the WRI World Congress on Computer Science and Information Engineering

[19] Brode, H.L. (1959). Blast wave from a spherical charge, The Physics of Fluids", 2(2), March/ April,